

Stress changes from the 2008 Wenchuan earthquake and increased hazard in the Sichuan basin

Tom Parsons¹, Chen Ji² & Eric Kirby³

On 12 May 2008, the devastating magnitude 7.9 (Wenchuan) earthquake struck the eastern edge of the Tibetan plateau, collapsing buildings and killing thousands in major cities aligned along the western Sichuan basin in China. After such a large-magnitude earthquake, rearrangement of stresses in the crust commonly leads to subsequent damaging earthquakes^{1–5}. The mainshock of the 12 May earthquake ruptured with as much as 9 m of slip along the boundary between the Longmen Shan and Sichuan basin, and demonstrated the complex strike–slip and thrust motion⁶ that

characterizes the region^{7,8}. The Sichuan basin and surroundings are also crossed by other active strike–slip and thrust faults. Here we present calculations of the coseismic stress changes that resulted from the 12 May event using models of those faults, and show that many indicate significant stress increases. Rapid mapping of such stress changes can help to locate fault sections with relatively higher odds of producing large aftershocks.

Globally, earthquakes like the magnitude (M) 7.9 shock that struck the western Sichuan region can be associated with triggered aftershocks⁵

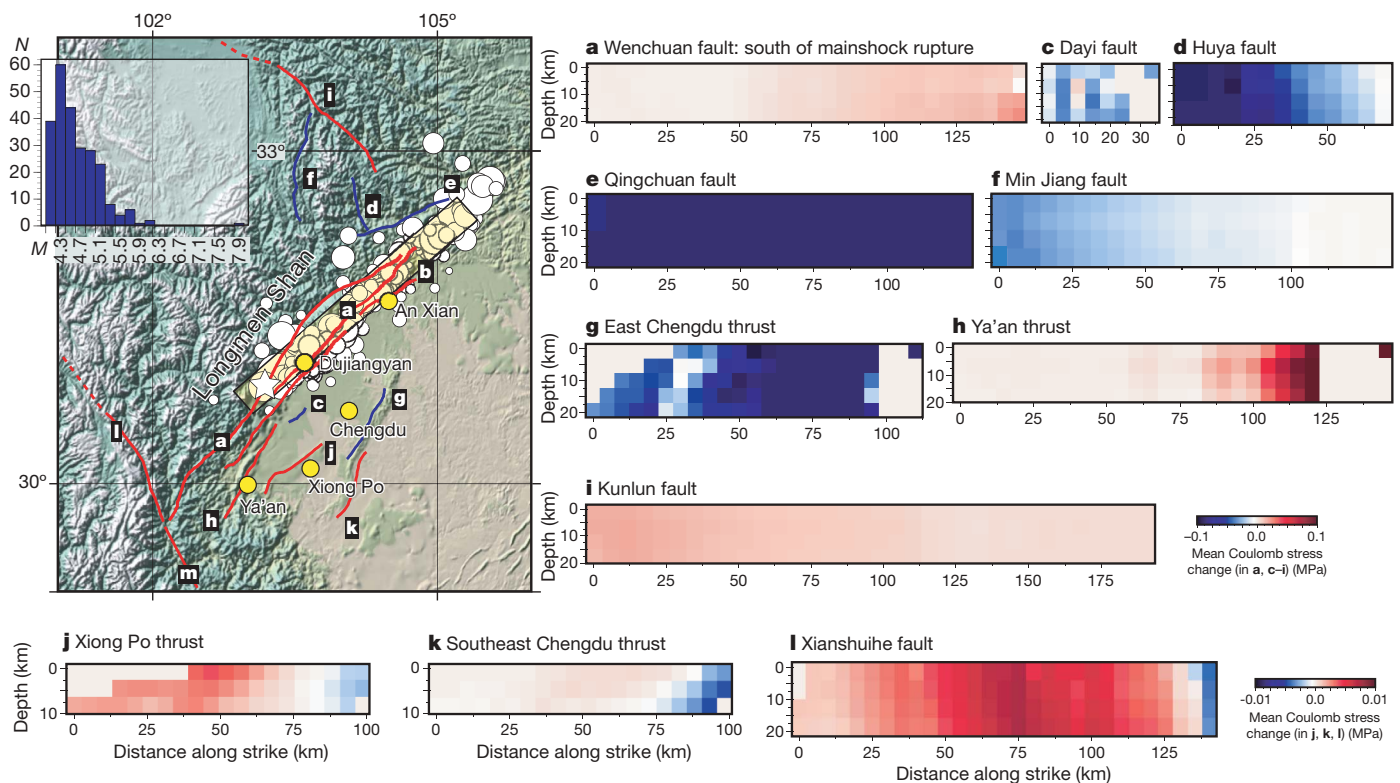


Figure 1 | Map of study area, calculated stress changes on major Sichuan basin and other faults after the Wenchuan earthquake, and aftershock data. Faults are labelled a–m in the map, and panels displaying calculated stress changes for most of these faults are shown; the zero of distance on each x axis marks the south end of the fault. Stress increases (>0.01 MPa) have been demonstrated to bring faults to failure, with delays ranging from seconds to decades^{2,5,12,13}. The epicentre is marked with a white star, aftershocks ($M \geq 4$) are shown as white circles, and the rupture plane is shown as an outlined yellow rectangle and coincides with a, the Beichuan and Wenchuan faults. The Wenchuan fault extends south of the rupture, and shows a calculated stress increase (data panel a). Whether b, the

Pengguan fault, was involved as well is uncertain, so no stress change calculations are shown for it. Most modelled faults show stress increases (red colours) except for c, Dayi, d, Huya, e, Qingchuan, f, Min Jiang, and g, the thrust east of Chengdu (blue shading). Note that the colour scales differ by region. The h, Ya'an thrust, i, Kunlun fault, j, Xiong Po thrust, k, thrust southeast of Chengdu, and l, the Xianshuihe fault all have calculated stress increases. Calculated stress changes on m, the Shimian fault, were negligible, so no data panel is shown for it. Yellow circles on the map indicate significant population centres. Map inset, aftershock magnitude–frequency ($M-N$) distribution as of 5 June 2008.

¹US Geological Survey, MS-999, 345 Middlefield Road, Menlo Park, California 94025, USA. ²Department of Geological Sciences, University of California, Santa Barbara, California 93106, USA. ³Department of Geosciences, Penn State University, University Park, Pennsylvania 16802, USA.

with $M > 7$; a recent example that affected a large population is the 1999 Izmit ($M = 7.4$) and Düzce ($M = 7.1$) pairing in Turkey. Stress-transfer analysis of those events came too late to be any factor for mitigation^{4,9}, but the technique was more successful after the great 2004 Sumatra earthquake, when a $M = 8.7$ shock struck three months later in a region calculated³ to have been stressed by the mainshock. For the 12 May 2008 event, early-stage calculations of coseismic stress transfer onto Sichuan basin faults are made by stepping through broad parameter ranges because exact values remain unknown. This approach enables rapid mapping of faults with heightened rupture likelihood (Fig. 1), and allows an opportunity for prospective testing of static stress transfer effects on earthquake hazard.

The 12 May $M = 7.9$ earthquake appears to have ruptured the Beichuan fault (labelled, together with the Wenchuan fault, as **a** in the map in Fig. 1) along the edge of the Longmen Shan (Fig. 1). The right-lateral oblique Pengguan fault^{7,8} (Fig. 1b) parallels the Beichuan fault, and it is unclear at the time of this writing whether this fault was directly involved in the mainshock rupture; if it was not involved, meaningful stress change calculations cannot be made on its surface because it is so close to the rupture¹⁰. Coulomb failure stress is calculated to have been increased south of the mainshock rupture on the Wenchuan fault (Fig. 1a) by up to 0.1 MPa. The active right-lateral⁸ strike-slip Dayi fault parallels the mainshock rupture, and as a result, is calculated to have reduced Coulomb stress (Fig. 1c). Thrust faults northwest of the rupture include the Huya, Qingchuan and Min Jiang zones¹¹ (Fig. 1d–f), and all indicate Coulomb stress reduction.

An array of thrust faults underlies the Sichuan basin, paralleling the range front (Fig. 1). These faults change in character from west to east across the basin; close to the range front, they dip to the northwest and appear to accommodate some right-lateral slip, whereas on the eastern side of the basin, faults dip shallowly down to the east^{7,8}. The thrust fault near Ya'an (Fig. 1h) lies south of the mainshock rupture and thus is calculated to have increased Coulomb stress. Similarly, the thrust faults bounding the Sichuan basin southeast of Chengdu (Fig. 1k) and near Xiong Po (Fig. 1j) also are calculated to have increased stress. Increases are calculated to be much smaller on the east side of the basin (~ 0.01 MPa) because they are located farther from the mainshock. The thrust fault immediately east of Chengdu (Fig. 1g) has a calculated stress decrease (about -0.01 MPa).

The Longmen Shan block is bound by left-lateral strike-slip faults to the north and south. The left-lateral Xianshuihe fault strikes northwest of its junction with the Wenchuan fault and has a calculated Coulomb stress increase over a 125-km length from the junction (Fig. 1l). South of the junction, left-lateral motion is taken up by the Shimian fault⁷ (Fig. 1m). Coulomb calculations on this segment show negligible changes. Similarly, calculations on the left-lateral Qinling fault, northeast of the Longmen Shan region, indicate negligible changes. However, the left-lateral Kunlun fault (Fig. 1i) northwest of the rupture shows a calculated stress increase. Thus it appears that most faults with calculated stress increases are confined to the southern Sichuan basin and boundaries, with the exception of the left-lateral Kunlun and Xianshuihe faults north and south of the basin.

The first 25-day period of aftershock activity ($M \geq 4$) is mostly confined within the mainshock rupture area (Fig. 1). The largest aftershocks within the period were two $M = 6$ events; the aftershock magnitude–frequency distribution (Fig. 1) suggests a potential moment deficiency in the $M = 5$ – 6.5 range, although variability is high and the number of events is small. Globally, static stress changes from $M > 7$ earthquakes are correlated with seismicity-rate changes over distances in excess of 200–250 km from the mainshock⁵.

The 12 May 2008 $M = 7.9$ earthquake that struck the eastern Sichuan region caused grievous losses, yet its legacy includes possible large aftershocks in the near future because it increased failure stress on important faults within and around the Sichuan basin. Given that delays of years to decades between mainshocks and large aftershocks are commonly observed around the world^{2,4}, identifying potential future rupture zones will be useful in focusing mitigation efforts.

Received 16 May; accepted 19 June 2008.

Published online 6 July 2008.

- Stein, R. S., Barka, A. A. & Dieterich, J. H. Progressive failure on the North Anatolian fault since 1939 by earthquake static stress triggering. *Geophys. J. Int.* **128**, 594–604 (1997).
- Stein, R. S. The role of stress transfer in earthquake occurrence. *Nature* **402**, 605–609 (1999).
- McCloskey, J., Nalbant, S. S. & Steacy, S. Indonesian earthquake: Earthquake risk from co-seismic stress. *Nature* **434**, 291 (2005).
- Parsons, T., Toda, S., Stein, R. S., Barka, A. & Dieterich, J. H. Heightened odds of large earthquakes near Istanbul: An interaction-based probability calculation. *Science* **288**, 661–665 (2000).
- Parsons, T. Global Omori law decay of triggered earthquakes: Large aftershocks outside the classical aftershock zone. *J. Geophys. Res.* **107**, doi:10.1029/2001JB000646 (2002).
- Ji, C. & Hayes, G. Preliminary result of the May 12, 2008 Mw 7.9 eastern Sichuan, China earthquake. (http://earthquake.usgs.gov/eqcenter/eqinthenews/2008/us2008ryan/finite_fault.php) (2008).
- Burchfiel, B. C., Chen, Z., Liu, Y. & Royden, L. H. Tectonics of the Longmen Shan and adjacent regions. *Int. Geol. Rev.* **37**, 661–735 (1995).
- Densmore, A. L. et al. Active tectonics of the Beichuan and Pengguan faults at the eastern margin of the Tibetan Plateau. *Tectonics* **26**, doi:10.1029/2006TC001987 (2007).
- Hubert-Ferrari, A. et al. Seismic hazard in the Marmara Sea region following the 17 August 1999 Izmit earthquake. *Nature* **404**, 269–273 (2000).
- Steacy, S., Marsan, D., Nalbant, S. S. & McCloskey, J. Sensitivity of static stress calculations to the earthquake slip distribution. *J. Geophys. Res.* **109**, doi:10.1029/2002JB002365 (2004).
- Kirby, E. & Whipple, K. X. Distribution of active rock uplift along the eastern margin of the Tibetan Plateau: Inferences from bedrock channel longitudinal profiles. *J. Geophys. Res.* **108**, doi:10.1029/2001JB000861 (2003).
- Harris, R. A. Introduction to special section: Stress triggers, stress shadows, and implications for seismic hazard. *J. Geophys. Res.* **103**, 24347–24358 (1998).
- Reasenber, P. A. & Simpson, R. W. Response of regional seismicity to the static stress change produced by the Loma Prieta earthquake. *Science* **255**, 1687–1690 (1992).

Supplementary Information is linked to the online version of the paper at www.nature.com/nature.

Acknowledgements We thank R. Harris and W. Thatcher for their help with this manuscript.

Author Information Reprints and permissions information is available at www.nature.com/reprints. Correspondence and requests for materials should be addressed to T.P. (tparsons@usgs.gov).